Proc. 29th IAHR Congress, Beijing, Theme E, Tsinghua Univers. Press, Beijing, pp. 365-373 (ISBN 7-302-04676-X/TV).

FLOW FIELD IN A TIDAL BORE: A PHYSICAL MODEL

H. Chanson

Department of Civil Engineering, The University of Queensland, Brisbane QLD 4072, Australia,
Fax: (61 7) 33 65 45 99, E-mail: h.chanson@mailbox.uq.edu.au

Abstract: A tidal bore may form in a converging channel with a funnel shape when the tidal range exceeds 6 to 9 m. The advancing surge has a major impact on the estuarine ecosystem. Physical modelling of an undular bore has been conducted based upon a quasi-steady flow analogy. The experimental data highlight rapid flow re-distributions between successive wave troughs and crests as well as large bottom shear stress variations. The results suggest a sediment transport process combining scour beneath wave troughs associated with upward matter dispersion between a trough and the following wave crest. The process is repeated at each undulation and significant sediment transport takes place with deposition in upstream intertidal zones. The conceptual model is supported by field observations showing murky waters after the bore passage and long-lasting chaotic waves.

Keywords: tidal bore, undular bore, undular jump, velocity, pressure, boundary shear stress, sediment process, mixing

1 INTRODUCTION

A bore is a positive surge of tidal origin which may form with large tidal ranges in a converging channel forming a funnel shape. The front of the surge absorbs random disturbances on both sides and this makes the wave stable and self-perpetuating. With appropriate boundary conditions, a tidal bore may travel long distances upstream: e.g., the tidal bore on the Pungue river (Mozambique) is still about 0.7 m high about 50 km upstream of the mouth and it may reach 80 km inland.

Tidal bores occur as the tidal flow turns to rising. As the surge progresses, the river flows upstream behind it (e.g. LYNCH 1982). Famous examples include the Hangzhou (or Hangchow) bore on the Qiantang river, the Amazon bore called *pororoca*, the tidal bore on the Seine river (*mascaret*) and the Hoogly (or Hooghly) bore on the Gange. Smaller tidal bores occur on the Severn river near Gloucester, England, on the Garonne and Dordogne rivers, France, at Turnagain Arm and Knik Arm, Cook Inlet (Alaska), in the Bay of Fundy (at Petitcodiac and Truro), on the Styx and Daly rivers (Australia), and at Batang Lupar (Malaysia) (Fig. 1).

A tidal bore may affect shipping industries. For example, the *mascaret* of the Seine river had had a sinister reputation. More than 220 ships were lost between 1789 and 1840 in the Quilleboeuf-Villequier section (MALANDAIN 1988). The height of the *mascaret* bore could reach up to 7.3 m and the bore front travelled at a celerity of about 2 to 10 m/s. Even in modern times, the Hoogly and Hangzhou bores are hazards for small ships and boats. The bore affects also the estuarine eco-system. The effect on sediment transport was studied at Petitcodiac and Shubenacadie rivers, on the Sée and Sélune (TESSIER and TERWINDT 1994) and on the Hangzhou bay (CHEN et al. 1990). The impact on the ecology is acknowledged in the Amazon where piranhas eat matter in suspension after the passage of the bore, at Turnagain Arm where bald eagles fish behind the bore, in the Severn river (sturgeons in the past, elvers) and in the Bay of Fundy (striped bass spawning).

Methodology

Despite their impact on estuarine processes, little is known on the flow field, mixing and sediment motion beneath tidal bores. Some salient characteristics of tidal bores are revealed in photographs of field occurrences : e.g., most tidal bores develop as undular surges. In absence of detailed field measurements and because numerical models based upon the Saint-Venant equations cannot handle free-surface undulations, a quasi-steady flow analogy was applied to investigate an undular tidal bore with the physical model of an undular jump.

The flow conditions were set as for the observations of the Severn bore by Captain BEECHEY on 1 December 1849 (TRICKER 1965). That is, $d_1 = 1.5$ m and $Fr_1 = 1.6$ where d_1 is the upstream water depth and Fr_1 is the bore Froude number. Dynamic similarity was achieved by selecting a Froude similitude (e.g. CHANSON 1999). Possible scale effects were investigated with two geometric scales: 18.7 and 32.6 (i.e. $d_1 = 0.080$ and 0.046 m respectively). Visually the river flow, before bore arrival, appears quiet, and the free-surface is smooth and glossy (e.g. Fig. 1B). In the model, the inflow turbulence level was minimised with a relatively small boundary layer thickness.

It is the purpose of this paper to gain a new understanding of the impact of undular tidal bores on river systems. The study is based upon experiments performed in a large-size facility with two geometric scaling ratios, associated with field observations.

2 EXPERIMENTAL INVESTIGATIONS

New experiments were performed in a rectangular horizontal channel. The flume (0.5-m wide, 3.2-m long) is made of smooth PVC bed and glass walls. The upstream supercritical flow is controlled by a sluice gate and the channel ends with an overflow gate.

The water discharge was measured with a Venturi meter, calibrated in-situ with a large V-notch weir. The percentage of error is expected to be less than 2%. The water depths were measured using a rail mounted pointer gauge. Pressure, velocity and bed shear stress distributions were recorded with a Prandtl-Pitot tube (3.35-mm external diameter, hemispherical nose). The translation of the gauge and Pitot tube in the direction normal to the channel bottom was controlled by a fine adjustment travelling mechanism (error less than 0.1 mm). The error on the transverse position of the gauge and tube is less than 0.5 mm and the error on their longitudinal position is less than 2 mm.

The Prandtl-Pitot tube was calibrated as a Preston tube based upon in-situ experiments and the calibration curve was best fitted by :

$$\tau_0 = 3.428 * V_b^{1.654} \qquad (1)$$

where τ_0 is the boundary shear stress and V_b is the velocity measured by the Pitot tube lying on the boundary (CHANSON 2000). The data accuracy is expected to be about 2% on dynamic and static pressures, 1% on local velocity and 5% on boundary shear stress.

For each experiment, the supercritical inflow was partially-developed : i.e., $\delta/d_1 \sim 0.4$ where δ is the boundary layer thickness and d_1 is the upstream water depth (Table 1). The upper fluid layer was nearly an ideal flow characterised by low turbulence level.

3 EXPERIMENTAL RESULTS

Visual observations and detailed measurements show that the undular jump is basically two-dimensional for $-0.42 < z/B < 0.42$, where z is the transverse distance measured from the centreline and B is the channel width (Table 2). Small sidewall cross waves were seen upstream of each wave crest. For both experiments, a large recirculation bubble was observed below the first crest, extending over most of the channel breadth with a maximum height of about $0.47*d_c$ (Fig. 2). Such a recirculation region was reported by other researchers investigating undular jumps with partially-developed inflow (see review in CHANSON and MONTES 1995).

Figure 3 presents dimensionless pressure and velocity distributions. The data are compared with an inviscid solution of the Boussinesq equation (MONTES and CHANSON 1998). Beneath the undulations, the pressure distributions are not hydrostatic. The pressure gradients are larger than hydrostatic when the free-surface is curved upwards (i.e. *concave*) and less than hydrostatic when *convex*. The trend is predicted by the irrotational flow motion theory (e.g. ROUSE 1938, LIGGETT 1994), although greater deviations from hydrostatic pressure distributions are experimentally observed (Fig. 3). The velocity distributions at the first wave crest differ considerably from theoretical predictions. Further downstream, the agreement between data and theory improves slightly. Nearly-identical results were obtained for both experiments in terms of velocity and pressure distributions, but very close to the sidewalls, suggesting that scale effects are negligible.

Dimensionless bottom boundary shear stress data are presented in Figure 4, where d_c and V_c are the critical depth and velocity respectively. The results show maximum boundary shear stresses below wave troughs and minimum values below the crests. Note that the data beneath the first wave crest were affected by the recirculation region (Fig. 2). Large longitudinal variations of shear stress are observed beneath the undulations : e.g., the boundary shear stress below the second trough is about twice of that observed at the second and third wave crest.

4 DISCUSSION

Applications to tidal bores

Considering an undular tidal bore progressing upstream, the river bed is subjected to a rapid flow reversal at the wave front associated with bottom shear stress reversal and maximum (negative) boundary shear stress beneath the troughs (Fig. 4 and 5). This pattern suggests some scour beneath wave troughs while sediment matter is carried upwards by vertical flow motion occurring between a trough and the following wave crest. For example, experimental data and ideal flow calculations yield depth-average vertical velocity component of about $+0.12*V_c$ between trough and crest. Further scour and sediment dispersion continue beneath the following undulations. Fine sediments (silt, clay) are put into suspension and transported upstream with the bore. Ultimately they are deposited in intertidal zones.

The writer observed the tidal bore of the Dordogne river at St Pardon (France) about 103 km upstream of Pointe de Grave on 27 September 2000 (coefficient: 103). At that location, the river is about 350 m wide and there is no sharp bend for about 3 to 4 km. The initial water depth was about 1.5 to 2 m. In September 2000, the bore exhibited about 8 to 12 well-formed undulations (wave height ~ 1 m, wave length ~ 8 m, Fr_1 ~ 1.3) followed by chaotic waves (Fig. 1). Two dominant features of the bore were the murkiness of the water after the passage of the bore, suggesting significant sediment motion, and the chaotic wave motion lasting for some time, making difficult for surfers to come back on shore even 20 minutes after the passage of the bore.

Although the latter effect was not documented, some researchers observed similar chaotic wave motion propagating as far as $(x-x_1)/d_c$ ~ 2,000 downstream of undular jumps in laboratory and in man-made canals (e.g. DARCY and BAZIN 1865, CHANSON 1995).

Limitations of the physical model

The application of the undular jump results has some limits. During the experiments, very rapid changes in velocity and pressure distributions were observed upstream of and at the first wave crest. A number of researchers reported similar observations in undular hydraulic jumps and it was demonstrated that the flow field is strongly affected by bottom and sidewall boundary friction (e.g. MONTES and CHANSON 1998). It is felt that the shear-dominated flow redistribution at the first wave crest is likely to be specific to undular hydraulic jumps and it might not be observed in undular positive surges.

5 SUMMARY AND CONCLUSION

The occurrence of tidal bores has a significant impact on river ecosystems. Physical modelling of an undular bore has been conducted based upon a quasi-steady flow analogy for two geometric scales. The experimental data highlight rapid pressure and velocity re-distributions between successive wave crests and troughs, and large longitudinal variations of bottom shear stress. The results suggest that bed erosion and scour take place beneath wave troughs, and that matters are carried upwards between a trough and the following wave crest (Fig. 5). The process is repeated at each undulation and it contributes to significant sediment transport with deposition in upstream intertidal areas. Such a model is confirmed by field observations showing murky waters after the bore passage. Long-lasting chaotic waves are also observed behind the bore and these contribute to further dispersion of sediments.

Acknowledgements

The writer acknowledges the assistance of K. HICKOX, C. QUINLAN and Y.H. CHOU (Australia). He thanks also Dr S. AOKI (Japan), Dr J.E. JONES (UK), Mr D. THIEDERMANN (USA), the Bore Ryders Club (UK) and many more people for providing him with new material of interest.

References

[1] CHANSON, H. (1995). "Flow Characteristics of Undular Hydraulic Jumps. Comparison with Near-Critical Flows." Report CH45/95, Dept. of Civil Engrg, Univ. of Queensland, Australia, 202 p.

[2] CHANSON, H. (1999). "The Hydraulics of Open Channel Flows : An Introduction." Butterworth-Heinemann, London, UK, 512 pages.

[3] CHANSON, H. (2000). "Boundary Shear Stress Measurements in Undular Flows : Application to Standing Wave Bed Forms." Water Res. Res., Vol. 36 , No. 10 , p. 3063.

[4] CHANSON, H., and MONTES, J.S. (1995). "Characteristics of Undular Hydraulic Jumps. Experimental Apparatus and Flow Patterns." Jl of Hyd. Engrg., ASCE, Vol. 121, No. 2, pp. 129.

[5] CHEN, J., LIU, C., ZHANG, C., and WALKER, H.J. (1990). "Geomorphological Development and Sedimentation in Qiantang Estuary and Hangzhou Bay." Jl of Coastal Res., Vol. 6, No. 3, pp. 559.

[6] DARCY, H.P.G., and BAZIN, H. (1865). "Recherches Hydrauliques." Imprimerie Impériales, Paris, France, Parties 1ère et 2ème.

[7] LIGGETT, J.A. (1994). "Fluid Mechanics." McGraw-Hill, New York, USA.

[8] LYNCH, D.K. (1982). "Tidal Bores." Scientific American, Vol. 247, No. 4, Oct., pp. 134-143.

[9] MALANDAIN, J.J. (1988). "La Seine au Temps du Mascaret." Le Chasse-Marée, No. 34, pp. 30-45.

[10] MONTES, J.S., and CHANSON, H. (1998). "Characteristics of Undular Hydraulic Jumps. Results and Calculations." Jl of Hyd. Engrg., ASCE, Vol. 124, No. 2, pp. 192-205.

[11] ROUSE, H. (1938). "Fluid Mechanics for Hydraulic Engineers." McGraw-Hill Publ., New York.

[12] TESSIER, B., and TERWINDT, J.H.J. (1994). "An Example of Soft-Sediment Deformations in an intertidal Environment - The Effect of a Tidal Bore". Comptes-Rendus de l'Académie des Sciences, Série II, Vol. 319, No. 2, Part 2, pp. 217-233.

[13] TRICKER, R.A.R. (1965). "Bores, Breakers, Waves and Wakes." American Elsevier Publ. Co., New York, USA.

Table 1 Experimental flow conditions

Reference	Fr_1	x_1	d_1	δ/d_1	Remarks
Present study					B = 0.5 m. Horizontal channel.
Exp. No. 1	1.58	0.3	0.046	0.43	Sluice gate opening : 70 mm.
Exp. No. 2	1.57	0.45	0.080	0.42	Sluice gate opening : 122.3 mm.

Table 2 Free-surface profile : Experiment No. 2

x (m)	d (m) z = 0 (CL)	d (m) z/B=0.144	d (m) z/B=0.284	d (m) z/B=0.438	Remarks
0.45	0.080	0.079	0.079	0.078	Upstream cross-section
1.20	0.097	0.093	0.091	0.092	Start of sidewall cross wave
1.27	0.125	0.123	0.125	0.137	
1.43	0.158	0.157	0.167	0.150	At 1st wave crest
1.60	0.133	0.127	0.124	0.133	
1.77	0.105	0.108	0.111	0.113	At 1st trough
1.91	0.131	0.126	0.124	0.121	
2.06	0.170	0.174	0.175	0.159	At 2nd crest
2.20	0.135	0.136	0.133	0.138	
2.34	0.117	0.115	0.113	0.115	At 2nd trough
2.47	0.130	0.135	0.137	0.131	
2.60	0.169	0.161	0.161	0.164	At 3rd crest

Fig. 1 Undular tidal bore of the Dordogne river on 27 Sept. 2000 at 5:00 pm (Photograph by the author) : (B) Looking upstream at the murky waters after the bore passage (foreground) and the glossy free-surface in background

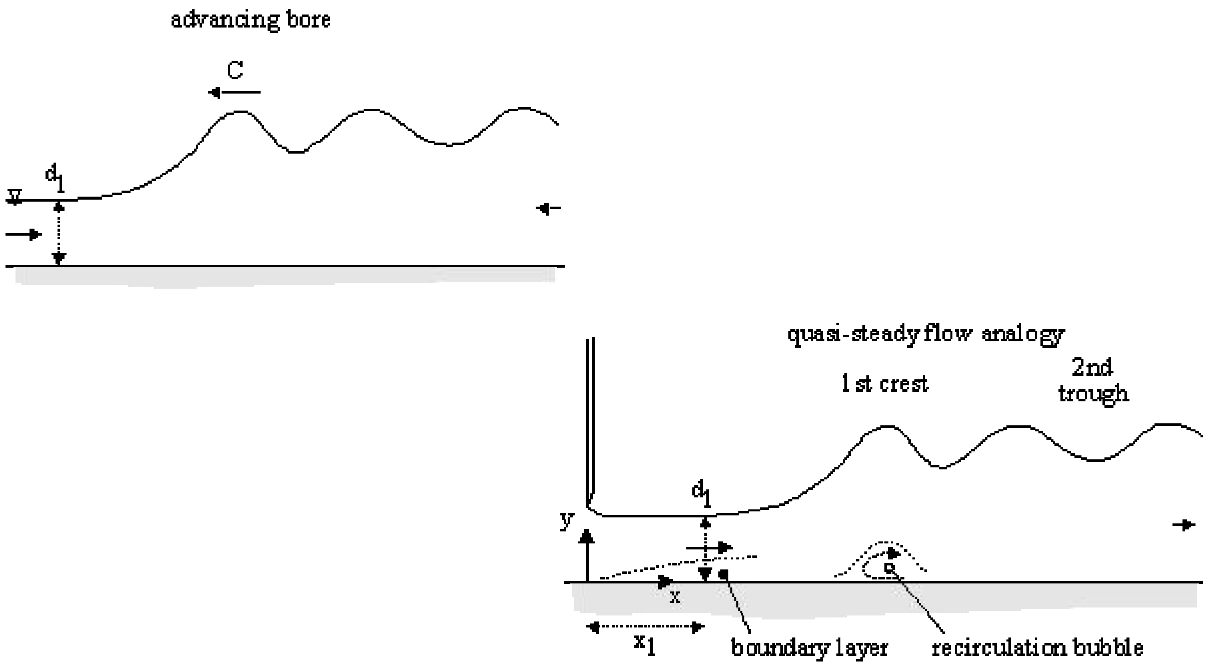

Fig. 2 Definition sketch

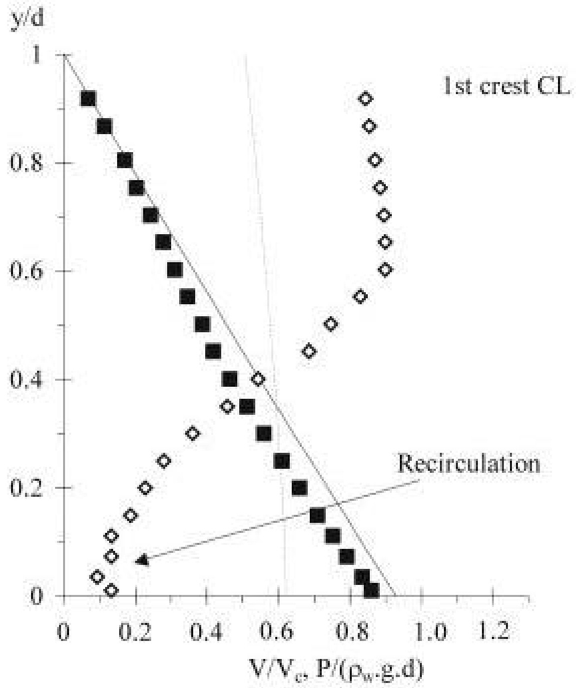

(A) First wave crest

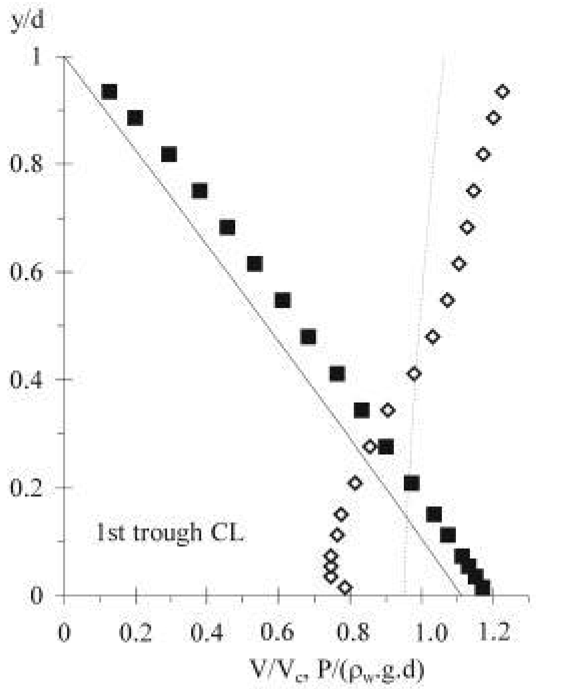

(B) First wave trough

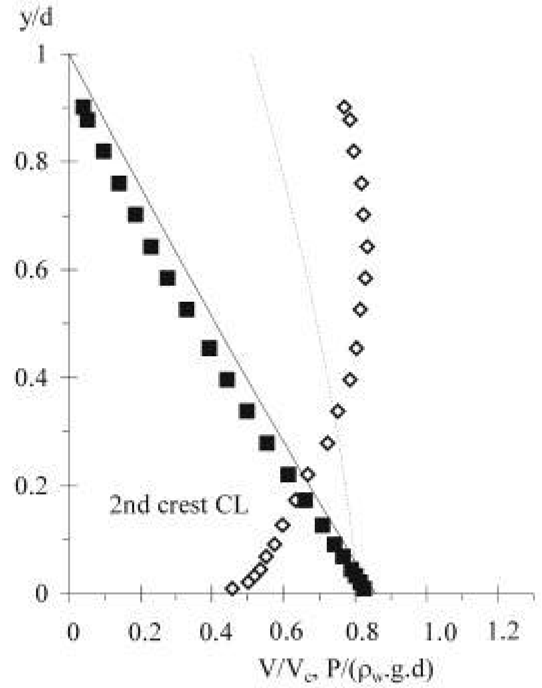

(C) Second wave crest

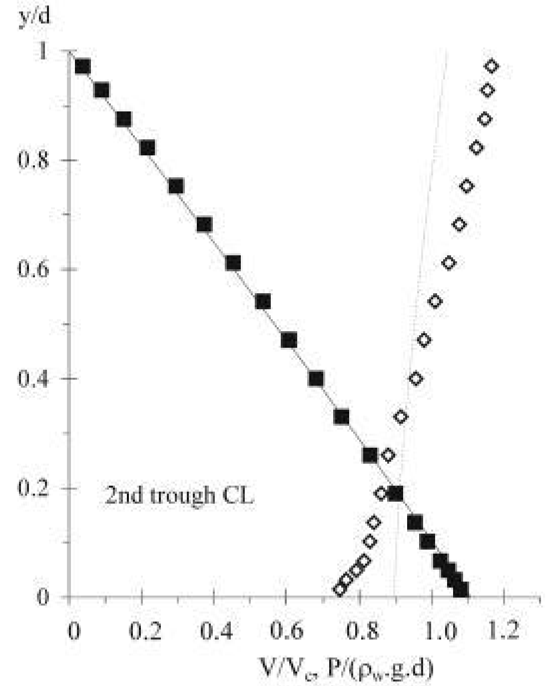

(D) Second wave trough

Fig. 3 Dimensionless pressure and velocity distributions : comparison with inviscid Boussinesq theory (MONTES and CHANSON 1998) - Exp. No. 2 centreline data
Legend : Black square = P/ρ_w*g*d; White diamond = V/V_c

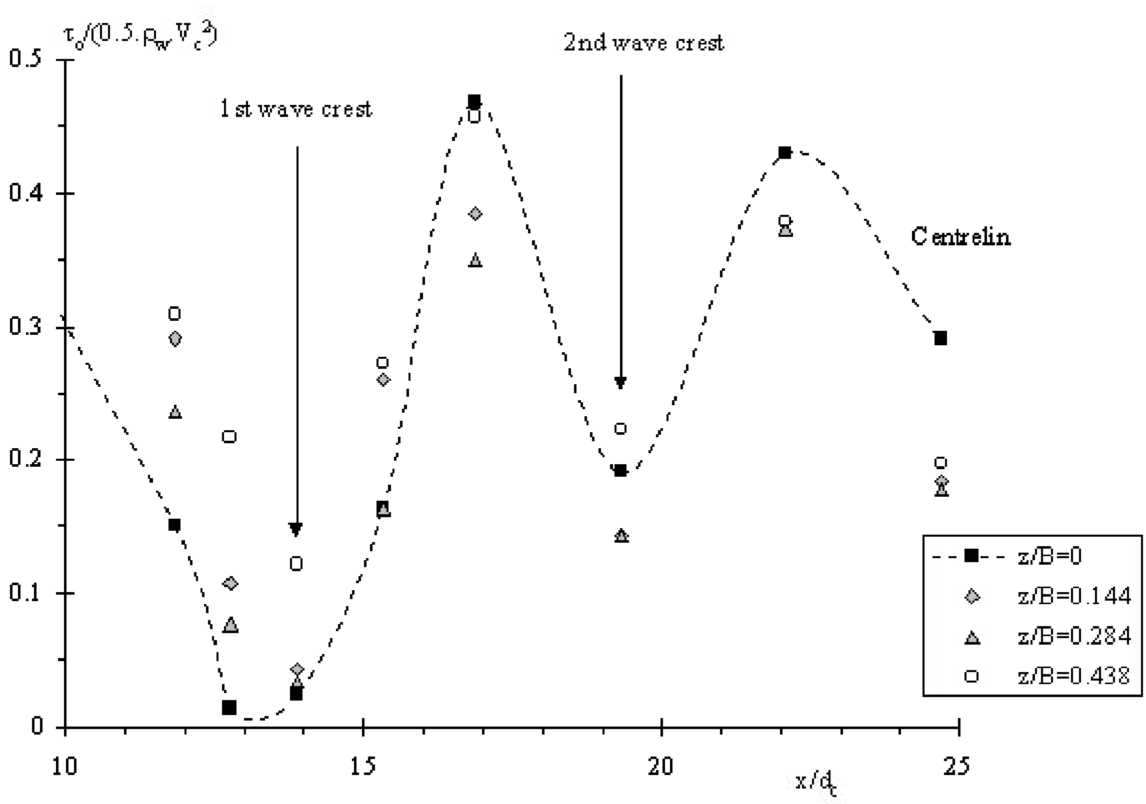

Fig. 4 Dimensionless bottom boundary shear stress $\tau_o/(\rho_w * V_c^2/2)$ as a function of the dimensionless longitudinal distance x/d_c(Exp. No. 2)

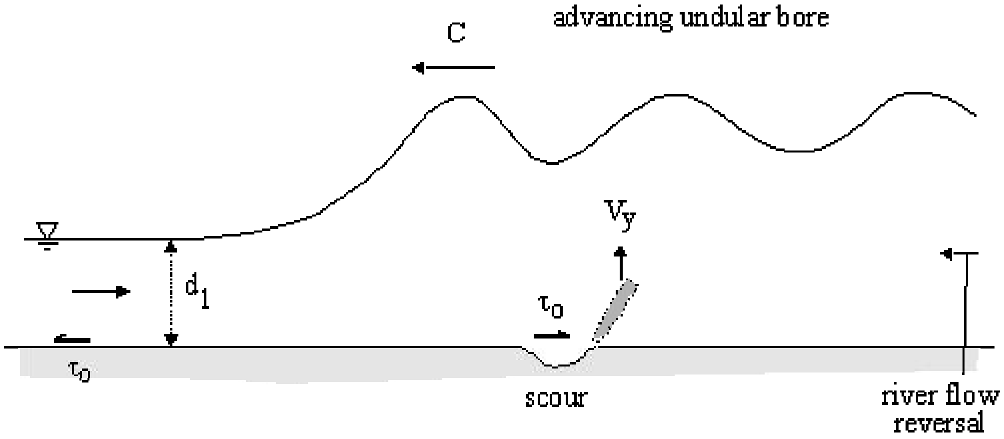

Fig. 5 Sketch of sediment bed scour and dispersion at an undular tidal bore